

New constraints on supersymmetric models from $b \rightarrow s\gamma$

F. Mahmoudi¹

High Energy Physics, Uppsala University, Box 535, 751 21 Uppsala, Sweden

Abstract

We provide an analysis of the parameter space of several supersymmetry breaking scenarios such as the minimal supergravity (mSUGRA) model and the non universal Higgs model (NUHM) framework, as well as the Anomaly Mediated Supersymmetry Breaking (AMSB) and the Gauge Mediated Supersymmetry Breaking (GMSB) models, in the light of a novel observable in $b \rightarrow s\gamma$ transitions, *i.e.* the isospin symmetry breaking in the exclusive $B \rightarrow K^*\gamma$ decay. We find that in many cases, this new observable provides severe restrictions on the allowed parameter space regions for the mentioned models. Moreover, we provide a few examples of investigations of the physical masses of supersymmetric particles and search for the excluded values. The constraints from the branching ratio associated to $b \rightarrow s\gamma$ are also presented here for all the examined parameter space regions. A comparison with $B_s \rightarrow \mu^+\mu^-$ branching ratio has also been performed.

PACS numbers: 11.30.Pb, 12.15.Mm, 12.60.Jv, 13.20.He

1 Introduction

During the last few years, constraints from the branching ratio of $b \rightarrow s\gamma$ have been extensively used as a guide for supersymmetry phenomenology and in particular, to constrain the MSSM [1]. Indeed, since these decays can only occur at loop level in the Standard Model, they bring very restrictive constraints on the new physics parameters.

In this study, we focus on a novel observable in $b \rightarrow s\gamma$ transitions, namely the isospin asymmetry, and show that this new observable can provide additional information to the inclusive branching ratio and, in some regions, even more restrictive limits on the SUSY parameters.

¹Electronic address: nazila.mahmoudi@tsl.uu.se

The isospin asymmetry for the exclusive process $B \rightarrow K^* \gamma$ is defined as

$$\Delta_{0-} = \frac{\Gamma(\bar{B}^0 \rightarrow \bar{K}^{*0} \gamma) - \Gamma(B^- \rightarrow K^{*-} \gamma)}{\Gamma(\bar{B}^0 \rightarrow \bar{K}^{*0} \gamma) + \Gamma(B^- \rightarrow K^{*-} \gamma)} , \quad (1)$$

and similarly Δ_{0+} is defined as the charge conjugate of this equation.

Using QCD factorization, one can show that the isospin asymmetry can be written as [2]:

$$\Delta_{0-} = \text{Re}(b_d - b_u) , \quad (2)$$

where the spectator-dependent coefficients b_q reads:

$$b_q = \frac{12\pi^2 f_B Q_q}{\bar{m}_b T_1^{B \rightarrow K^*} a_7^c} \left(\frac{f_{K^*}^\perp}{\bar{m}_b} K_1 + \frac{f_{K^*} m_{K^*}}{6\lambda_B m_B} K_{2q} \right) . \quad (3)$$

In this equation, a_7^c , K_1 and K_{2q} depend on the Wilson coefficients. We adopt here the definitions and conventions of [3] for the different parameters appearing in Eq. (3). An analysis of the branching ratio and isospin symmetry breaking in the context of beyond QCD factorization has also been performed in [4].

The experimental data for exclusive decays from Babar [5] and Belle [6] point to isospin asymmetries of at most a few percent:

$$\Delta_{0-} = +0.050 \pm 0.045(\text{stat.}) \pm 0.028(\text{syst.}) \pm 0.024(R^{+/0}) \quad (\text{Babar}) , \quad (4)$$

$$\Delta_{0+} = +0.012 \pm 0.044(\text{stat.}) \pm 0.026(\text{syst.}) \quad (\text{Belle}) . \quad (5)$$

Calculating the expected isospin asymmetry from Eqs. (2) and (3), and confronting the results to the combined experimental limits of (4) and (5) allow us to establish limits on the supersymmetry parameters. In [3], we have detailed the calculation of the isospin asymmetry in the MSSM with minimal flavor violation, and performed scans on the mSUGRA parameter space. This study extends the analysis of [3] to a broader range of supersymmetric hypotheses, and we investigate the constraints from the isospin asymmetry for different scenarios of supersymmetry breaking. As a comparison reference, we also calculate the inclusive branching ratio associated to $b \rightarrow s \gamma$.

All the calculations in this paper, for both the inclusive branching ratio and the isospin symmetry breaking have been performed using the computer program SuperIso [7], which is a public C program which calculates the isospin asymmetry, using a SUSY Les Houches Accord file for the input parameters, that can be either automatically generated thanks to for example SOFTSUSY [8] or ISAJET [9], or provided by the user.

In the following sections, after deriving the bounds on the isospin asymmetry and estimating the errors, we give a summary of the results in the minimal supergravity (mSUGRA) parameter space, and we present the constraints from isospin asymmetry for other scenarios such as non universal Higgs model (NUHM), the Anomaly Mediated Supersymmetry Breaking (AMSB) and the Gauge Mediated Supersymmetry Breaking (GMSB) models.

| CKM parameters and B meson mass | | | | |
|---------------------------------|--------------------------------------|--------------------------------------|--|----------------------------------|
| V_{us} | V_{cb} | $ V_{ub}/V_{cb} $ | $\text{Re}(V_{us}^* V_{ub}/V_{cs}^* V_{cb})$ | m_B |
| 0.22 | 0.041 ± 0.05 | 0.085 ± 0.025 | 0.011 ± 0.005 | 5.28 GeV |
| B meson parameters | | | | |
| f_B | λ_B | a_\perp | $\langle \bar{v}^{-1} \rangle_\perp$ | $h_{K^*}(x)$ |
| 200 ± 20 MeV | 350 ± 150 MeV | 0.19 ± 0.02 | 3.7 ± 0.04 | $(4.8 \pm 0.5) + (1.5 \pm 0.2)i$ |
| K^* meson parameters | | | | |
| $f_{K^*}^\perp$ | m_{K^*} | f_{K^*} | $T_1^{B \rightarrow K^*}$ | |
| 175 ± 9 MeV | 892 MeV | 226 ± 28 MeV | 0.30 ± 0.05 | |
| Convolution integral parameters | | | | |
| F_\perp | $G_\perp(x_{cb})$ | $H_\perp(x_{cb})$ | X_\perp | |
| 1.21 ± 0.06 | $(2.82 \pm 0.20) + (0.81 \pm 0.23)i$ | $(2.32 \pm 0.16) + (0.50 \pm 0.18)i$ | $(3.44 \pm 0.47) X - (3.91 \pm 1.08)$ | |
| Quark and W -boson masses | | | | |
| $m_b(m_b)$ | $m_c(m_b)$ | m_s | m_t | M_W |
| 4.2 ± 0.1 GeV | 1.2 ± 0.2 GeV | 0.10 ± 0.03 GeV | 172.5 ± 2.7 GeV | 80.4 GeV |

Table 1: Numerical values of the parameters involved in the calculation of the isospin asymmetry. The parameter $X = \ln(m_B/\Lambda_h) (1 + \varrho e^{i\varphi})$ parametrizes the logarithmically divergent integral $\int_0^1 dx/(1-x)$.

2 Bounds on isospin asymmetry

In this section, we perform a general analysis of the errors, in order to derive the effective bounds on the isospin asymmetry.

The calculation of Δ_{0-} requires the knowledge of many parameters (please refer to [2, 3] for a complete description of the calculation), whose values and associated errors are given in Table 1¹.

Allowing as usual $\varrho \leq 1$ and an arbitrary phase φ , we perform an analysis of the errors due to the variation of the input parameters of Table 1. We find, at 95% C.L., that the total relative theoretical error is about 35%. The highest relative uncertainties arise from λ_B (10%), $T_1^{B \rightarrow K^*}$ (7%), f_B (3%), and X (3%).

¹Most of the values in this table are taken from [10] and [11], with some updates.

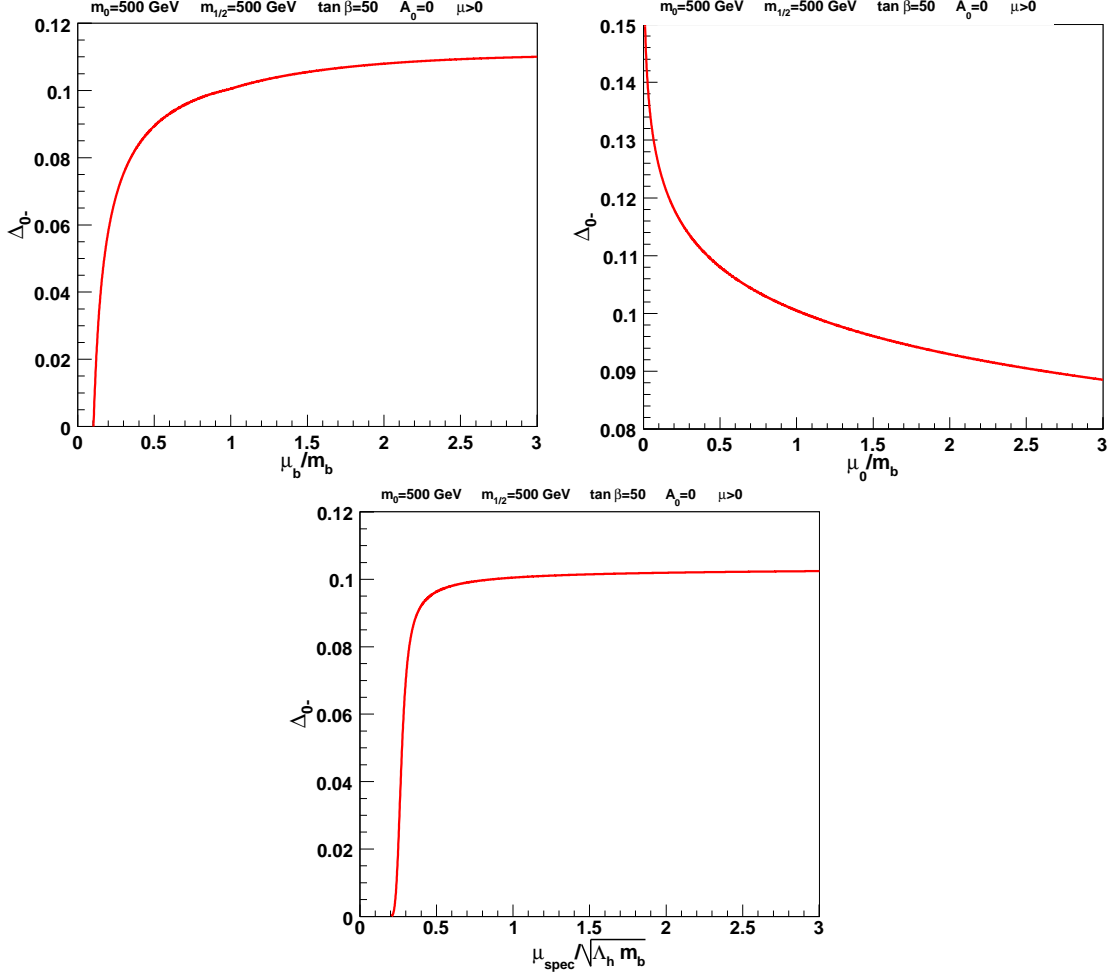


Figure 1: Dependence of the isospin asymmetry on the scales μ_b , μ_0 and μ_{spec} . We consider here the mSUGRA parameter space with $m_0 = 500$ GeV, $m_{1/2} = 500$ GeV, $\tan \beta = 50$, $A_0 = 0$ and $\mu > 0$.

However, the isospin asymmetry calculation also involves the choice of three different scales, $\mu_b = O(m_b)$, $\mu_0 = O(m_b)$ and $\mu_{spec} = O(\sqrt{\Lambda_h m_b})$, where Λ_h is a hadronic scale that we take to be approximately 0.5 GeV. The dependence of the theoretical predictions on the choice of the scales can be considered as an estimate of higher-order corrections. This dependence is depicted in Fig. 1. We can first remark that Δ_{0-} is quite stable with respect to the variation of μ_{spec} . We can also observe a higher scale dependence of Δ_{0-} for small values of the μ 's. Following the usual practice, we evaluate the truncation errors while varying the scales μ_b , μ_0 and μ_{spec} independently, in the ranges $\mu_b \in [m_b/2, 2m_b]$, $\mu_0 \in [m_b/2, 2m_b]$ and $\mu_{spec} \in [\sqrt{\Lambda_h m_b}/2, 2\sqrt{\Lambda_h m_b}]$, with their central values taken to be respectively m_b , m_b and $\sqrt{\Lambda_h m_b}$. We then calculate the truncation error of the sum by adding the individual errors in quadrature. In this manner, we

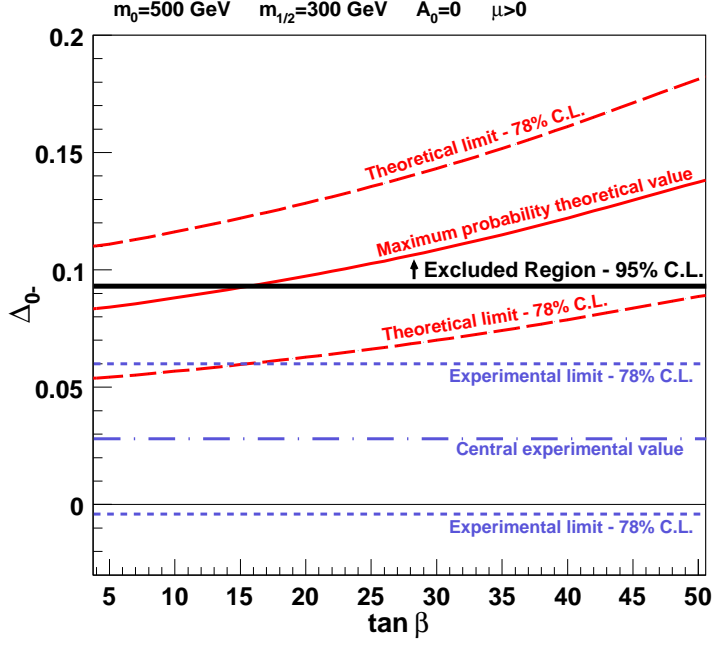


Figure 2: Evaluation of the experimental and theoretical errors, in the mSUGRA parameter space with $m_0 = 500 \text{ GeV}$, $m_{1/2} = 300 \text{ GeV}$, $A_0 = 0$ and $\mu > 0$. The horizontal black line corresponds to the criterion (6), which is a 95% confidence level limit, to be compared with the red straight line corresponding to the calculated isospin asymmetry.

determine the relative uncertainty corresponding to the choice of the scales: -15% / + 10%. This error can be considered as an evaluation of the influence of higher order contributions. Combining all the sources of errors, we find that the total relative theoretical uncertainty at 95% C.L. is -50% / +45%.

Combining the experimental and the theoretical errors, we derive the criterion (at 95% C.L.):

$$-0.018 < \Delta_{0-} < 0.093 \quad . \quad (6)$$

This criterion is illustrated in Fig. 2. The upper limit will be used in the following sections to impose constraints on supersymmetric parameter spaces. Although the uncertainties are very large, we can safely claim that the theoretical values for the isospin asymmetry should not exceed 9.3% (at 95% C.L.), and this allows us to rule out models (or parameters) which produce too large isospin asymmetry.

3 Isospin asymmetry and the MSSM

In this section, a comparison between the theoretical evaluation and the experimental bounds of the last section has been performed. We investigate the constraints from the isospin asymmetry for several scenarios of supersymmetry breaking.

3.1 mSUGRA

A more detailed investigation of the minimal supergravity model (mSUGRA) parameter space has been presented in [3, 12]. Here we emphasize only an example of the major results of the former articles, and we do also some comparisons with other B Physics observables.

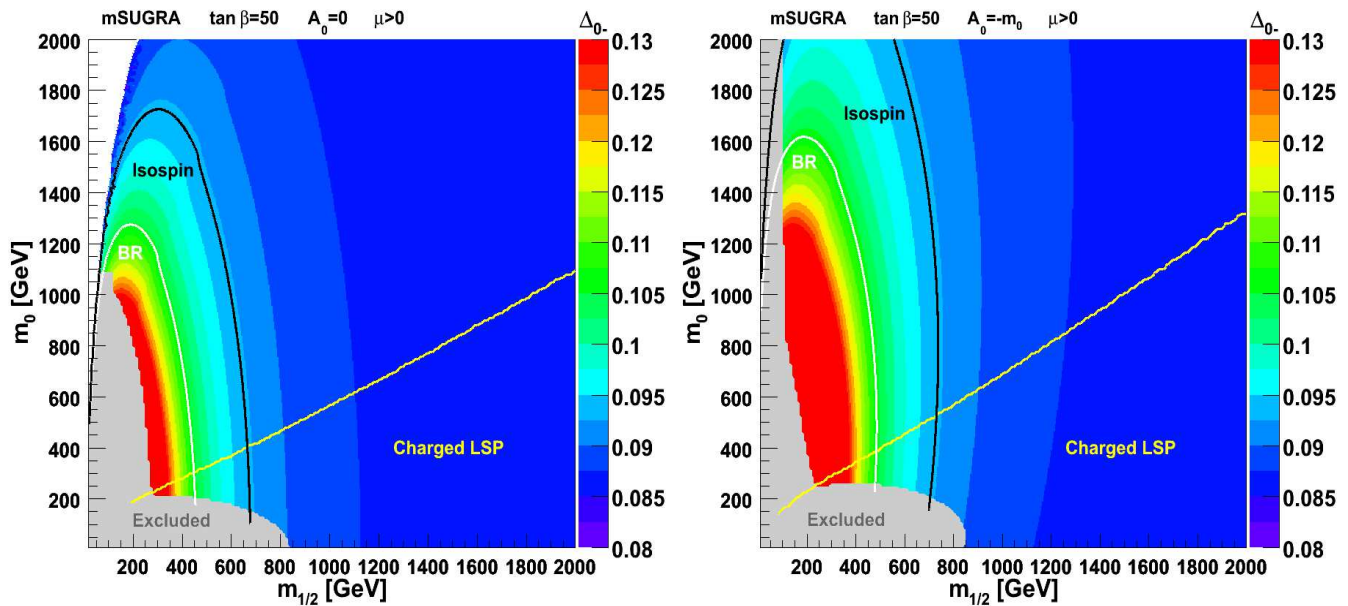


Figure 3: Constraints on the mSUGRA parameter plane $(m_{1/2}, m_0)$ for $A_0 = 0$ (left) and $A_0 = -m_0$ (right). The conventions for the colors and the meaning of the different regions are described in the text.

The SUSY mass spectrum, as well as the couplings and the mixing matrices have been generated using SOFTSUSY 2.0.14 [8].

We scan the mSUGRA parameter space $\{m_0, m_{1/2}, A_0, \tan\beta, \text{sign}(\mu)\}$, and for every point we calculate the isospin asymmetry and confront it to the limits of Eq. (6). We also calculate

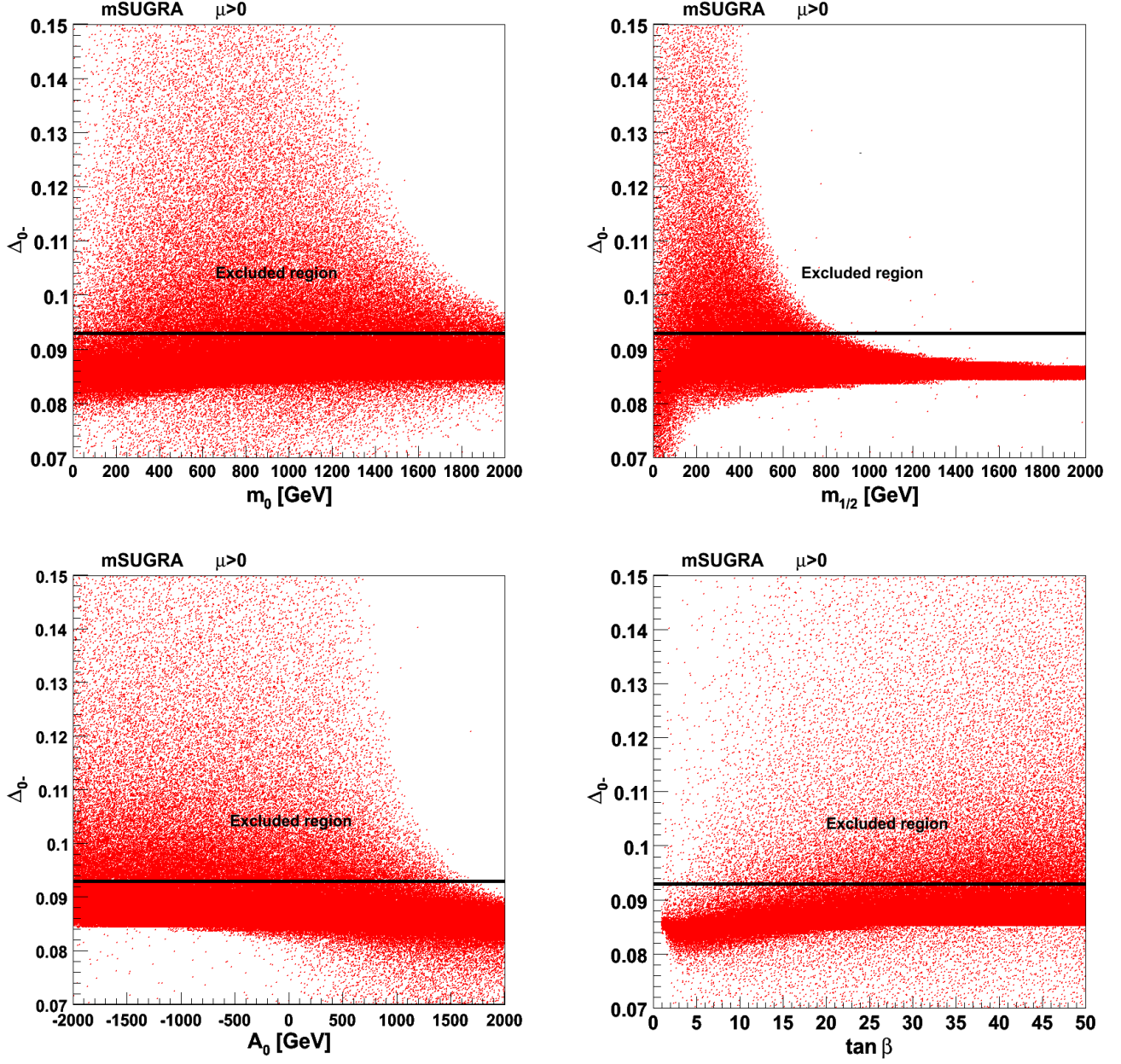


Figure 4: Dependence of isospin symmetry breaking on the different input parameters of the mSUGRA model, when scanning over one million randomly chosen parameter space points, for $\mu > 0$.

the inclusive branching ratio as a comparison reference. For the branching ratio, the following limits (at 95% C.L.) have been used [13]:

$$2.33 \times 10^{-4} < \mathcal{B}(b \rightarrow s\gamma) < 4.15 \times 10^{-4} . \quad (7)$$

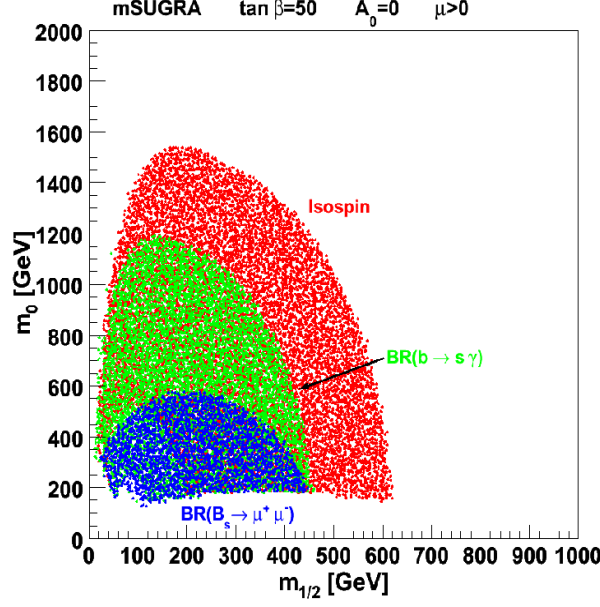


Figure 5: Excluded regions in the mSUGRA parameter plane $(m_0, m_{1/2})$ for $\tan\beta = 50$ and $A_0 = 0$. The red region is excluded by the isospin asymmetry of $B \rightarrow K^*\gamma$, while the green region is excluded by the inclusive branching ratio of $B \rightarrow X_s\gamma$. The blue region is excluded by the branching ratio of $B_s \rightarrow \mu^+\mu^-$.

In Fig. 3, an investigation of the $(m_{1/2}, m_0)$ plane for $A_0 = 0$ and $A_0 = -m_0$ is presented. In this figure, the black contour marked “Isospin” delimits the region excluded by the isospin breaking constraints, whereas the contour marked “BR” corresponds to the region excluded by the inclusive branching ratio constraints. The “Excluded” area in the figure corresponds to the case where at least one of the sparticle masses does not satisfy the collider constraints or where the neutral Higgs boson becomes too light [14]. Finally, the “Charged LSP” region is cosmologically disfavored if R-parity is conserved. The various colors represent the changing magnitude of the isospin asymmetry.

One can notice the severe constraints from the isospin symmetry breaking, especially for large $\tan\beta$ values and for $\mu > 0$. One can also note that the isospin asymmetry is enhanced by a negative value of A_0 , although the global shapes of the limiting regions remain similar.

In order to have a better idea of the dependence of isospin asymmetry on different mSUGRA parameters, we present in Fig. 4 the results of the scan over one million randomly chosen parameter space points while varying the mSUGRA input parameters in the ranges $m_0 \in [0, 2000]$, $m_{1/2} \in [0, 2000]$, $A_0 \in [-2000, 2000]$ and $\tan\beta \in [0, 50]$, for $\mu > 0$. The horizontal black line in this figure corresponds to the limit of Eq. (6). One can notice here a larger number of excluded points for higher values of $\tan\beta$, small values of $m_{1/2}$ and negative values of A_0 . Approximately 10% of the analyzed points are in the excluded region.

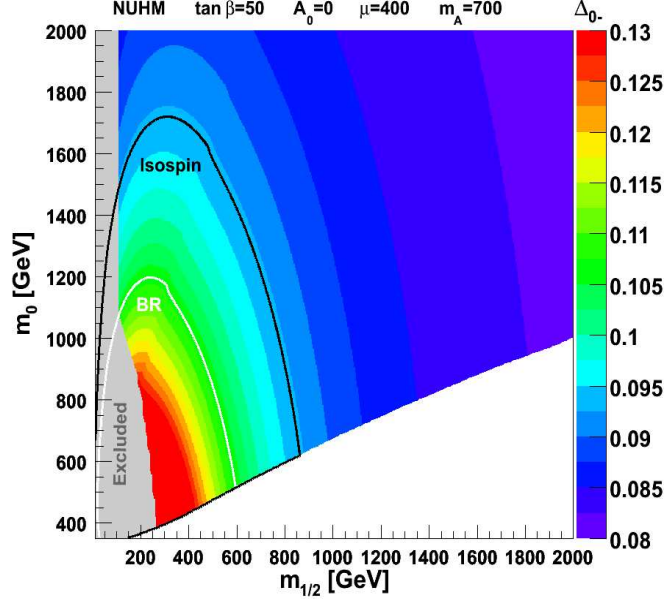


Figure 6: Constraints on the NUHM parameter plane $(m_{1/2}, m_0)$ for $A_0 = 0$. The conventions for the different colored regions are the same as in Fig. 3. In the white region tachyonic particles are encountered.

To evaluate how restrictive the isospin symmetry breaking is compared to the other B Physics observables, we show in Fig. 5 an example of the regions excluded by the branching ratio of $B_s \rightarrow \mu^+ \mu^-$ (in blue), by the inclusive branching ratio of $B \rightarrow X_s \gamma$ (in green) and by the isospin asymmetry of $B \rightarrow K^* \gamma$ (in red), for $\tan \beta = 50$ and $A_0 = 0$.

We can remark that isospin asymmetry is more constraining than both the branching ratio observables.

For this plot, we used the following constraint for the branching ratio of $B_s \rightarrow \mu^+ \mu^-$ [15]:

$$\mathcal{B}(B_s \rightarrow \mu^+ \mu^-) < 0.97 \times 10^{-7} , \quad (8)$$

and the masses and couplings were generated using ISAJET 7.75 [9].

In this section, we showed that in the studied mSUGRA regions, the isospin asymmetry greatly enlarges the exclusion contours compared to the previously used B physics observables.

3.2 NUHM

We explore in this section the non universal Higgs model (NUHM) parameter space [16], in which the universality assumptions of the soft SUSY breaking contributions to the Higgs masses

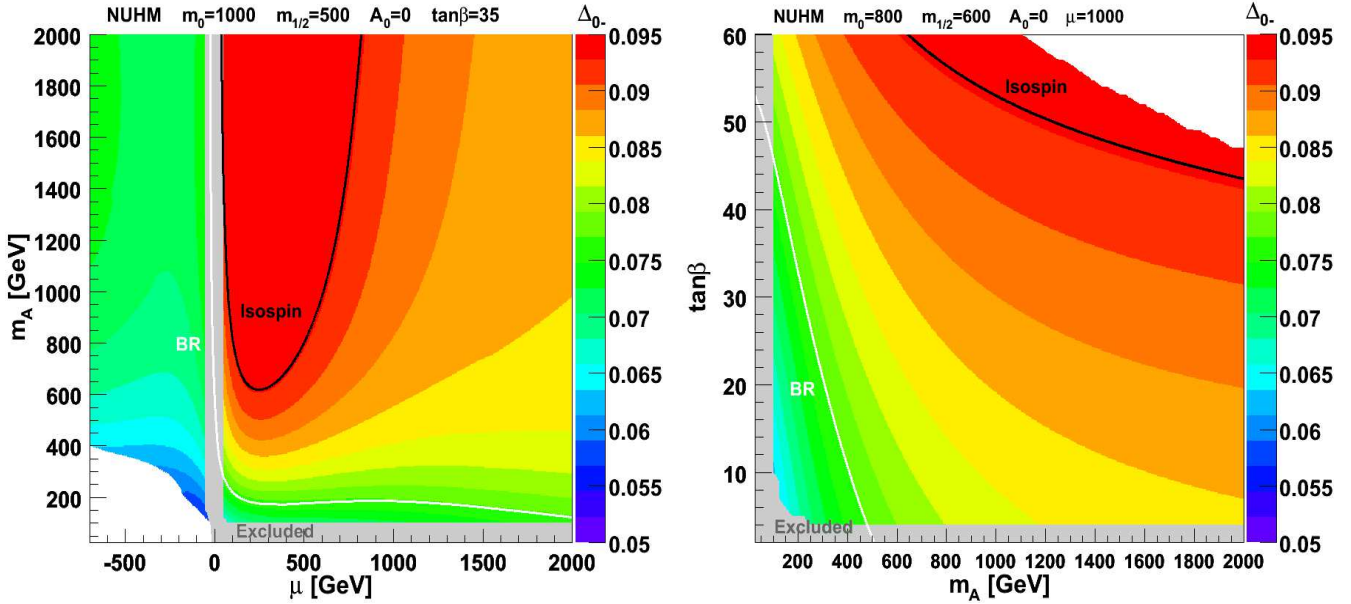


Figure 7: Constraints on the NUHM parameter planes, (μ, m_A) to the left and $(m_A, \tan \beta)$ to the right. The white BR contour delimits the region excluded by the branching ratio, and the black contour corresponds to the isospin symmetry breaking constraint. The conventions for the different regions are the same as in the precedent figures, but the color scale here is different.

are relaxed as compared to the mSUGRA scenario. Within this framework, two additional free parameters, M_A and μ , add to the five universal parameters of the mSUGRA scenario.

Fig. 6 shows an example of the results in the $(m_{1/2}, m_0)$ plane for $\tan \beta = 50$, $A_0 = 0$, $M_A = 700$ GeV and $\mu = 400$ GeV. The masses and couplings have been generated using SOFTSUSY 2.0.14 [8]. The results are similar to those for the mSUGRA parameter space, as was expected. The white area at the lower part of this figure has not been generated since it corresponds to tachyonic particles.

In Fig. 7, the (μ, m_A) and $(m_A, \tan \beta)$ planes have been investigated. For these two samples, the regions excluded by the branching ratio and by the isospin asymmetry are not correlated anymore. One can thus appreciate the additional information provided by this new observable. Furthermore, these results can be compared to other existing constraints, for example those from WMAP. For instance, comparing the (μ, m_A) plane (Fig. 7) with a similar plot presented in [17], one can notice that the WMAP favored region was between two strips at roughly constant positive and negative values of μ , extending approximately to $\mu = 350$ GeV. It is remarkable that the isospin asymmetry constraint reduces a substantial part of this region. This is a nice example to illustrate the usefulness of exploring new observables such as isospin asymmetry

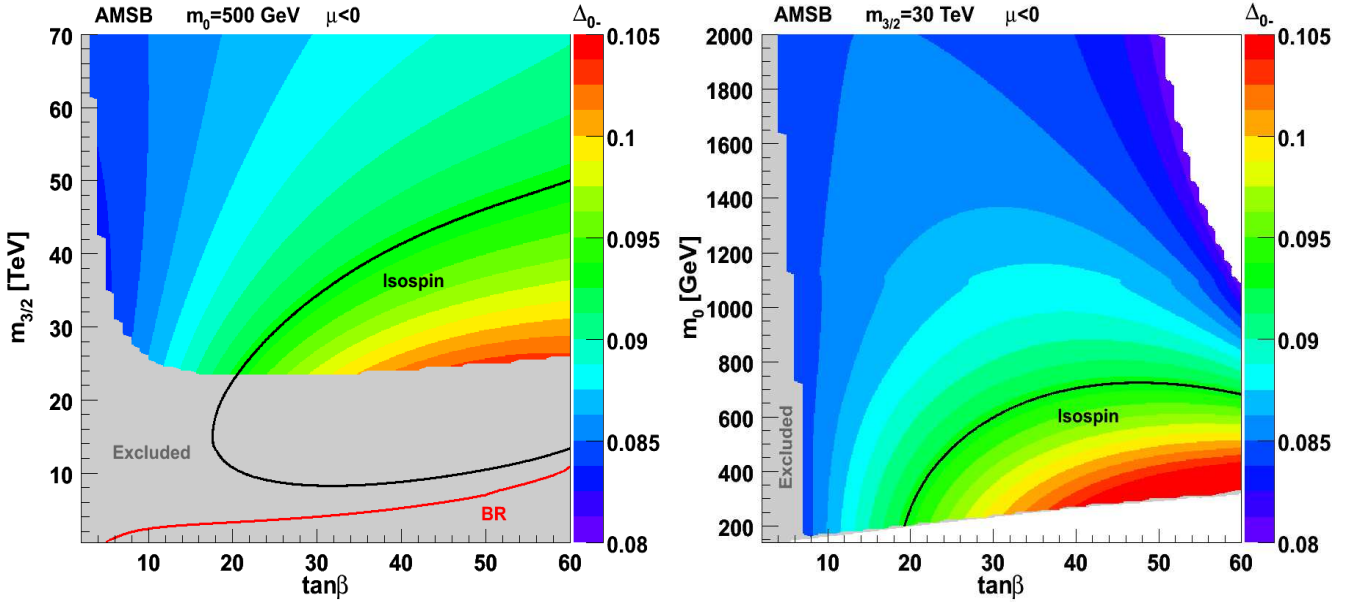


Figure 8: Constraints on the AMSB parameter planes $(\tan\beta, m_{3/2})$ and $(\tan\beta, m_0)$. The conventions for the different regions are the same as in the precedent figures.

and the complementary information one can obtain.

3.3 AMSB

We can now focus on other supersymmetry breaking scenarios, and study the influence of the isospin asymmetry for these models. First we consider the Anomaly Mediated Supersymmetry Breaking (AMSB) scenario [18]. These mechanisms are well motivated since they preserve virtues of the gravity mediated models while the FCNC problem is solved.

For this scenario, we generate the masses and couplings with SOFTSUSY 2.0.14 [8], and perform scans in the parameter space $\{m_0, m_{3/2}, \tan\beta, \text{sign}(\mu)\}$.

The results are presented in Fig. 8, where the $(\tan\beta, m_{3/2})$ and $(\tan\beta, m_0)$ planes have been studied.

For the $(\tan\beta, m_{3/2})$ plane, the constraints from the branching ratio are in the region already excluded by the collider mass limits. In the $(\tan\beta, m_0)$ plane, we obtain no limit from the branching ratio. However, for both cases, we obtain remarkable contours from the isospin asymmetry. This is another example in favor of investigating the isospin symmetry breaking observable.

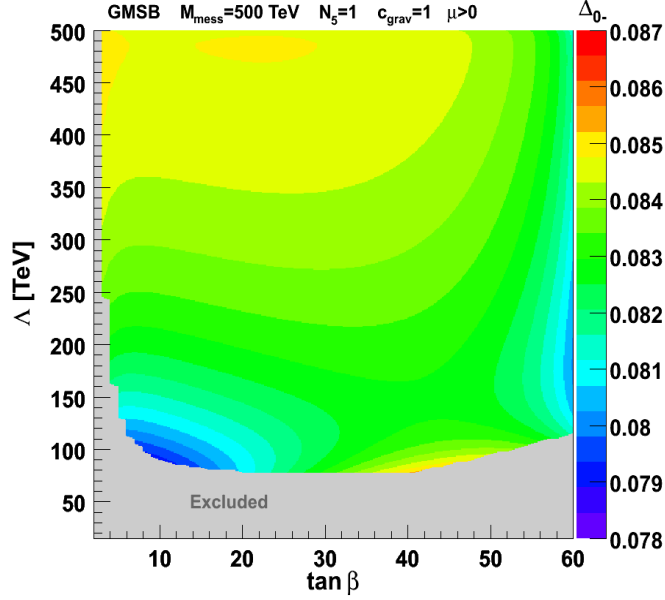


Figure 9: Evolution of the isospin asymmetry in the GMSB parameter plane $(\tan \beta, \Lambda)$.

3.4 GMSB

As a final example, we consider the Gauge Mediated Supersymmetry Breaking (GMSB) scenario [19]. Several regions in the parameter space $\{\Lambda, M_{\text{mess}}, N_5, c_{\text{grav}}, \tan \beta, \text{sign}(\mu)\}$ have been investigated. Unfortunately, the available experimental data do not allow us to obtain any constraints from neither the branching ratio nor the isospin symmetry breaking.

Nevertheless, to show how the isospin asymmetry evolves in the GMSB parameter space, we perform a scan for $M_{\text{mess}} = 500$ TeV, $N_5 = 1$ and we set $c_{\text{grav}} = 1$. The masses and couplings have been generated with SOFTSUSY 2.0.14 [8]. Fig. 9 shows the results for the $(\tan \beta, \Lambda)$ plane.

With more accurate experimental data becoming available, one can hope that the isospin asymmetry could be a valuable observable also in this scenario.

3.5 Physical constraints

Up to this point, we investigated the dependence of the isospin symmetry breaking on the parameters of different supersymmetry breaking models. We now consider the physical masses of the superpartners and investigate the values excluded by the isospin and branching ratio constraints.

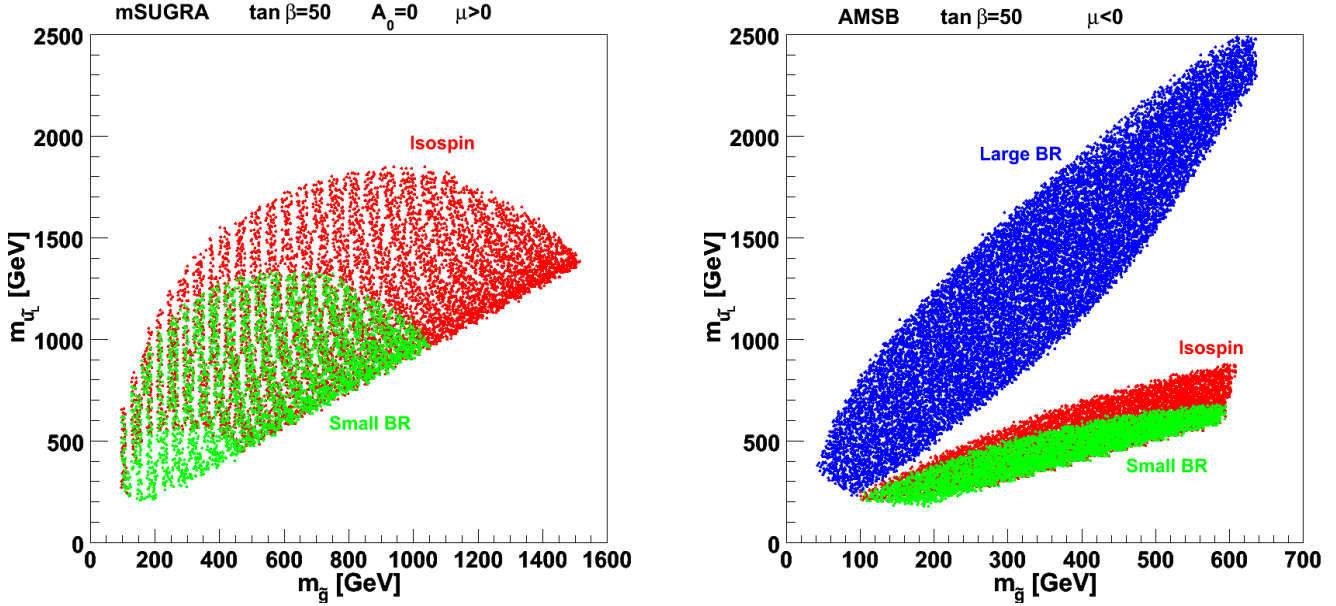


Figure 10: The mSUGRA parameter space to the left for $\tan\beta = 50$ and $A_0 = -m_0$. To the right, the AMSB parameter space for $\tan\beta = 50$. The red dotted regions are excluded by isospin asymmetry constraints, while the green regions are excluded by the lower bound on the branching ratio and the blue region by the upper bound on the branching ratio.

We consider first the masses of gluinos and squarks, which are relevant for the strong interaction phenomenology. For this purpose, we explore mSUGRA and AMSB parameter spaces and we consider \tilde{u}_L squark as an example, since all heavy squarks have approximately the same mass. The results of the scans for $(m_{\tilde{g}}, m_{\tilde{u}})$ planes are shown in Fig. 10. We generated the masses and couplings using SOFTSUSY 2.0.14 [8]. The regions excluded by isospin symmetry breaking are marked with red dots, while those excluded by the branching ratio are marked with blue and green dots. The region with approximately $m_{\tilde{u}_L} > 0.8m_{\tilde{g}}$ is not accessible due to the fact that squarks can become tachyonic at high scales in this region [20].

One can notice that in the AMSB parameter space, both the upper and lower bounds of the branching ratio provide restrictive constraints, but that the isospin asymmetry still rules out some additional parts of the space.

As another example, we study the constraints on the charged Higgs mass. The charged Higgs boson is of special interest as a new physics discovery channel at the LHC. Fig. 11 shows two dimensional plots illustrating the constraints on the charged Higgs mass from the isospin asymmetry in the mSUGRA parameter space. The calculation has been done for different values of $\tan\beta$. The horizontal line in these plots delimits the upper bound of the allowed isospin asymmetry. One can notice that the highest restrictions are obtained for large $\tan\beta$ values.

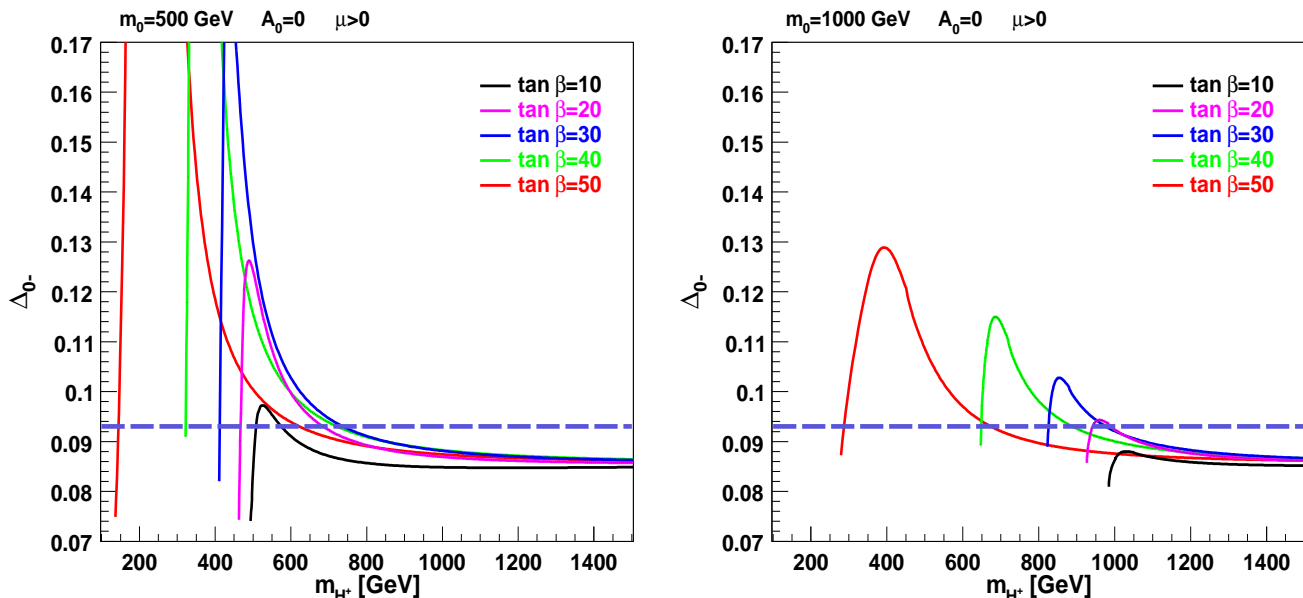


Figure 11: Constraints on the charged Higgs mass in the mSUGRA parameter space for $A_0 = 0$ and for different values of $\tan \beta$. The horizontal dashed line shows the limit from isospin asymmetry, ruling out all the region above it.

For instance, for $m_0 = 500$ and $\tan \beta = 50$, the mass range between approximately 150 GeV and 640 GeV is excluded, while for $\tan \beta = 30$, the region between roughly 400 GeV and 720 GeV is excluded. One can also notice that for a higher value of m_0 such as $m_0 = 1000$ GeV, only larger values of charged Higgs masses are excluded.

4 Summary

In this article, we explored different supersymmetric scenarios and presented the new information and constraints obtained from isospin symmetry breaking in radiative B meson decays. The calculations have been performed using our recently developed program SuperIso [7].

In many regions, the constraints from isospin symmetry breaking are very restrictive. Therefore, this new observable is very valuable to probe new physics scenarios. The study presented here is not exhaustive, and other regions/parameters, or models, could easily be explored by the same method. In this paper we have shown some examples of the information we can obtain

using this novel observable.

Finally, extending this study to other models, in particular beyond the MSSM could also be of interest.

Acknowledgments

I would like to thank Sven Heinemeyer for useful discussions. I am also grateful to Gunnar Ingelman, Johan Rathsman and Oscar Stål for helpful discussions and for their comments on the manuscript.

References

- [1] See for instance G. Isidori and P. Paradisi, Phys. Lett. **B639**, 499 (2006) [hep-ph/0605012], or J.R. Ellis, S. Heinemeyer, K.A. Olive, A.M. Weber and G. Weiglein, JHEP **0708**, 083 (2007) [arXiv:0706.0652].
- [2] A. Kagan and M. Neubert, Phys. Lett. **B539**, 227 (2002) [hep-ph/0110078].
- [3] M.R. Ahmady and F. Mahmoudi, Phys. Rev. **D75**, 015007 (2007) [hep-ph/0608212].
- [4] P. Ball, G.W. Jones and R. Zwicky, Phys. Rev. **D75**, 054004 (2007) [hep-ph/0612081].
- [5] B. Aubert *et al.* (BABAR Collaboration), Phys. Rev. **D70**, 112006 (2004) [hep-ex/0407003].
- [6] M. Nakao *et al.* (BELLE Collaboration), Phys. Rev. **D69**, 112001 (2004) [hep-ex/0402042].
- [7] F. Mahmoudi, arXiv:0710.2067, <http://www3.tsl.uu.se/~nazila/superiso/>.
- [8] B.C. Allanach, Comput. Phys. Commun. **143**, 305 (2002) [hep-ph/0104145].
- [9] H. Baer, F.E. Paige, S.D. Protopescu and X. Tata, hep-ph/0312045.
- [10] S.W. Bosch and G. Buchalla, JHEP **0501**, 035 (2005) [hep-ph/0408231].
- [11] A. Ali and A.Y. Parkhomenko, Eur. Phys. J. **C23**, 89 (2002) [hep-ph/0105302].
- [12] F. Mahmoudi and M.R. Ahmady, AIP Conf. Proc. **903**, 283 (2007) [hep-ph/0610144].
- [13] M. Battaglia *et al.*, Eur. Phys. J. **C22**, 535 (2001) [hep-ph/0106204].
- [14] W.-M. Yao *et al.* (Particle Data Group), J. Phys. **G33**, 1 (2006), <http://pdg.lbl.gov/>
- [15] V.M. Abazov *et al.* (D0 Collaboration), arXiv:0707.3997.

- [16] J.R. Ellis, K.A. Olive and Y. Santoso, Phys. Lett. B**539**, 107 (2002) [hep-ph/0204192].
- [17] J.R. Ellis, T. Hahn, S. Heinemeyer, K.A. Olive and G. Weiglein, arXiv:0709.0098.
- [18] For a review see K. Huitu, J. Laamanen and P.N. Pandita, Phys. Rev. D**65**, 115003 (2002) [hep-ph/0203186].
- [19] For a review see G.F. Giudice and R. Rattazzi, Phys. Rept. **322**, 419 (1999) [hep-ph/9801271].
- [20] U. Ellwanger, Phys. Lett. B**141**, 435 (1984).